CHAPTER

10

ANALYSIS OF DATA FROM ROCK-DEFORMATION EXPERIMENTS

Terry Engelder
Stephen Marshak

10-1 INTRODUCTION

Experimental rock deformation refers to the laboratory study of the mechanical characteristics of rocks. These characteristics include *rheology* (the response of rock to stress), *strength* (the maximum stress that can be sustained by a rock before it fails), and *friction* (the resistance to sliding on a fracture surface in the rock). In such work, specimens of rocks (usually machined cubes or cylinders) are subjected to measured stresses under varying conditions of temperature, confining pressure, strain rate, pore pressure, and chemical environment. Rock-deformation experiments can be used to model both *brittle deformation*, meaning deformation that involves formation of and movement on discrete fractures in a rock, and *ductile deformation*, meaning deformation that occurs without loss of cohesion across a plane. Structural geologists should be able to read and interpret descriptions of experiments, because experiments simulate deformation in the earth and therefore provide insight into the physical processes by which common structures, such as faults and folds, form.

Ideally, structural-geology students should have the opportunity to observe or participate in experimental studies. Unfortunately, most schools do not have the equipment to demonstrate such studies. The purpose of this chapter is to describe rock-deformation experiments and provide an opportunity to work with methods for representing and interpreting experimental results. The format of this chapter differs from that of previous chapters in that you are asked to work through the interpretations of the experiments that are outlined in the text. The discussion in this chapter is limited to certain types of rock-deformation experiments; we consider experiments concerning rock strength under brittle, brittle-ductile, and ductile conditions, and we consider experiments concerning rock friction. Ultimately, these experiments give information about the state of stress in the upper crust. To introduce the terminology of experimental rock deformation, we begin by describing some of the equipment used in rock-deformation experiments and by describing the diagrams commonly used to represent rock-deformation data.

10-2 THE ROCK-DEFORMATION EXPERIMENT

Experimental Apparatus

Many rock-deformation experiments are carried out on a *triaxial load machine* (Fig. 10-1). This device is a sophisticated press that is able to exert a stress on a rock cylinder or cube. Stress (force per unit area) is commonly measured in pascals (1 Pa = 1 X 10^{-5} kg m^{-1} s^{-2}), where 1 MPa = 10 bars = 145 psi (psi means "pounds per square inch"). The length/diameter ratio of rock cylinders used in experiments is generally around 2:1, and cylinders range in size from 5-mm diameter (small), through 2.5-cm diameter (standard), up to 30-cm diameter (large). Work with different size cylinders is important because strength is scale dependent. Larger cylinders are more likely to contain

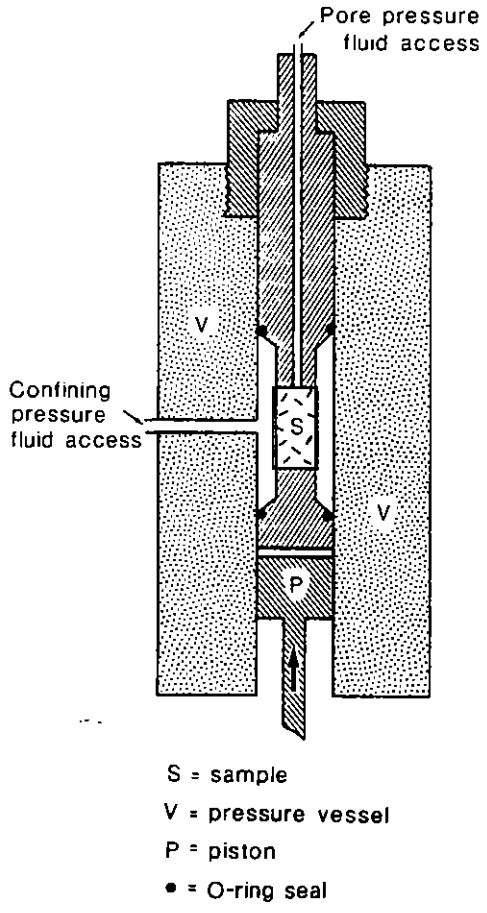

(a)

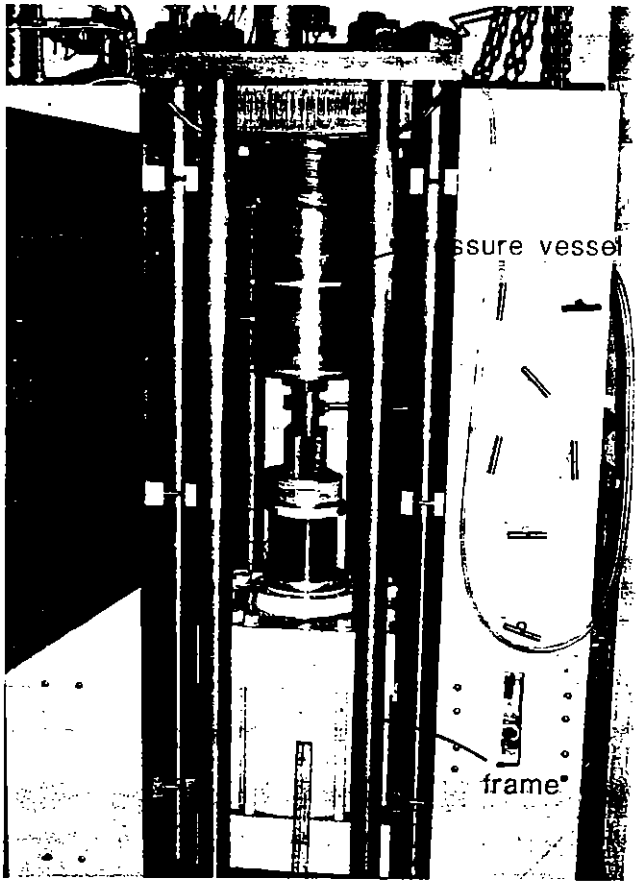

(b)

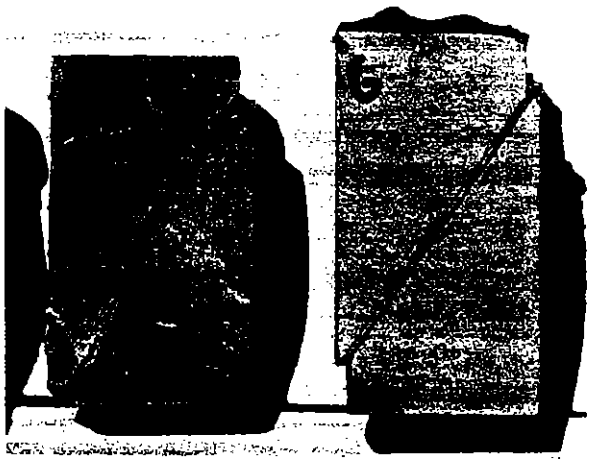

(c)

Figure 10-1. Triaxial load machine. (a) Diagrammatic cross-sectional sketch of a portion of a machine showing the pressure vessel, sample, and piston; (b) photograph of a machine; (c) photograph of two deformed samples. The left sample contains an induced fracture. The right sample contains a saw-cut for friction experiments. There is a 5 mm-thick layer of gouge along the cut. Samples are 3.5" long and 2" in diameter.

flaws such as microfractures that will cause local stress concentrations leading to failure (see Means, 1976, Jaeger and Cook, 1979, and Kulander et al., 1979 for further discussion of stress concentration).

During an experiment a rock cylinder is squeezed by displacement of a piston in the machine (Fig. 10-1). In response to the displacement of the piston, the axial length of the cylinder changes. This change, the *axial strain* of the cylinder, is measured by an electrical transducer attached to the cylinder. The axial stress felt by the cylinder during an experiment is measured by a load cell aligned with the piston and the cylinder.

Typically, a triaxial experiment is designed so that physical conditions can be varied during the experiment. For example, it is possible to control the following parameters:

Strain rate (the time rate of change of the rock-cylinder length), by specifying the rate at which the piston moves during the experiment.

Temperature, by heating the cylinder during an experiment.

Confining pressure (the pressure exerted on the sides of the cylinder), by placing the cylinder in a pressure vessel containing a confining medium (usually kerosene or argon). The pressure of the confining medium is controlled during the experiment. The cylinder is usually jacketed in copper, lead, or plastic to isolate it from the confining medium. A solid medium such as talc is sometimes used for very high pressure experiments.

Pore pressure (the pressure of the fluid that fills pores in the rock cylinder), by allowing fluid to reach the cylinder via small conduits in the machine (Fig. 10-1). The pressure of the fluid in the cylinder is regulated independently of the axial stress or of the pressure in the confining fluid.

The term triaxial refers to the fact that all three principal stresses (σ_1, σ_2, and σ_3) can be manipulated during an experiment, so that none is necessarily equal to atmospheric pressure in the laboratory. The subscript 1 signifies the maximum principal compressive stress, the subscript 2 signifies intermediate principal compressive stress, and the subscript 3 signifies the minimum principal compressive stress. If a rock cylinder is used, the axial stress is σ_1 in compression, and the confining pressure is σ_2 and σ_3 (σ_2 and σ_3 are equal because of the sample geometry and the experimental configuration). The *differential stress*, which is defined as the axial stress minus the confining pressure is,

$$\Delta\sigma = \sigma_1 - \sigma_3 \qquad \text{(Eq. 10-1).}$$

If the pore pressure (P_p) is not equal to 0, then the preceding equation may be rewritten in terms of *effective stress* ($^*\sigma_1$):

$$^*\sigma_1 \text{ (}\textit{effective axial stress}\text{)} = \sigma_1 - P_p \qquad \text{(Eq. 10-2)}$$

$$^*\sigma_3 \text{ (}\textit{effective confining pressure}\text{)} = \sigma_3 - P_p \qquad \text{(Eq. 10-3)}$$

and thus,

$$\Delta\sigma = {}^*\sigma_1 - {}^*\sigma_3 = \sigma_1 - \sigma_3 \qquad \text{(Eq. 10-4).}$$

Two basic experiments are possible with a triaxial load machine. The first type is called a *constant strain-rate experiment*. During such an experiment, as the name suggests, the piston of the machine moves at the same rate throughout the experiment. The second type is called a *constant stress experiment* (also called a *creep test*). During a creep test the stress is held constant, and a variation in strain rate is measured as a function of time. Creep tests are useful in constraining the *constitutive equations* (quite simply, equations that specify strain rate as a function of stress) associated with different deformation mechanisms. This chapter is restricted to descriptions of constant strain-rate experiments.

Representation of Data on Stress-Strain Plots

There are a number of ways to represent the results of rock-deformation experiments. Commonly, results are displayed on a *stress-strain plot*. A stress-strain plot is merely a graph, constructed in Cartesian coordinates, that plots differential stress (measured in bars, pascals, or other valid units) on the vertical axis against strain in a specified direction on the horizontal axis (Fig. 10-2). The direction of strain is usually parallel to the axis of the test cylinder. Remember that *strain* is defined as the ratio of change of length of line over the initial length; it is a dimensionless quantity usually represented by a percentage.

On a stress-strain plot the results of a constant strain-rate experiment involving *elastic* deformation plot as a straight line (portion of the curve labeled "elastic deformation" on Fig. 10-2a). The slope of this line is a rock property called *Young's modulus*. This straight-line relationship indicates that, for an elastically deforming material, strain is directly proportional to stress. The stress-strain relationship can be represented by the equation $\sigma = E\varepsilon$, where E is Young's modulus and ε is the strain.

It is commonly observed in rock-deformation experiments that a rock behaves elastically until a certain strain is achieved; then the rock either *fails* brittlely (i.e., it fractures, suddenly loses cohesion, and can no longer support the stress, so the stress drops; Fig. 10-2b, curve A), *yields* by fracture (rock does not necessarily lose all cohesion when it fractures), or deforms plastically. If the curve on a stress-strain plot still has a positive slope after yielding has occurred, the rock is said to exhibit *strain hardening* during deformation (Fig. 10-2b, curves F). If the curve has a negative slope after yielding, the rock is said to exhibit *strain softening* (Fig. 10-2b, curve D). A sample that yielded by fracture may fail after a certain amount of strain hardening or strain softening (Fig. 10-2b, curves B and C). *Perfectly plastic* behavior on a stress-strain plot is represented by a horizontal straight line once the rock yields (Fig. 10-2b, curve E). Such a plot means that, for a plastically deforming material, strain will continue to increase as long as the stress is held at or above the ultimate strength of the rock.

Elastic strain is *recoverable*, in that if stress is

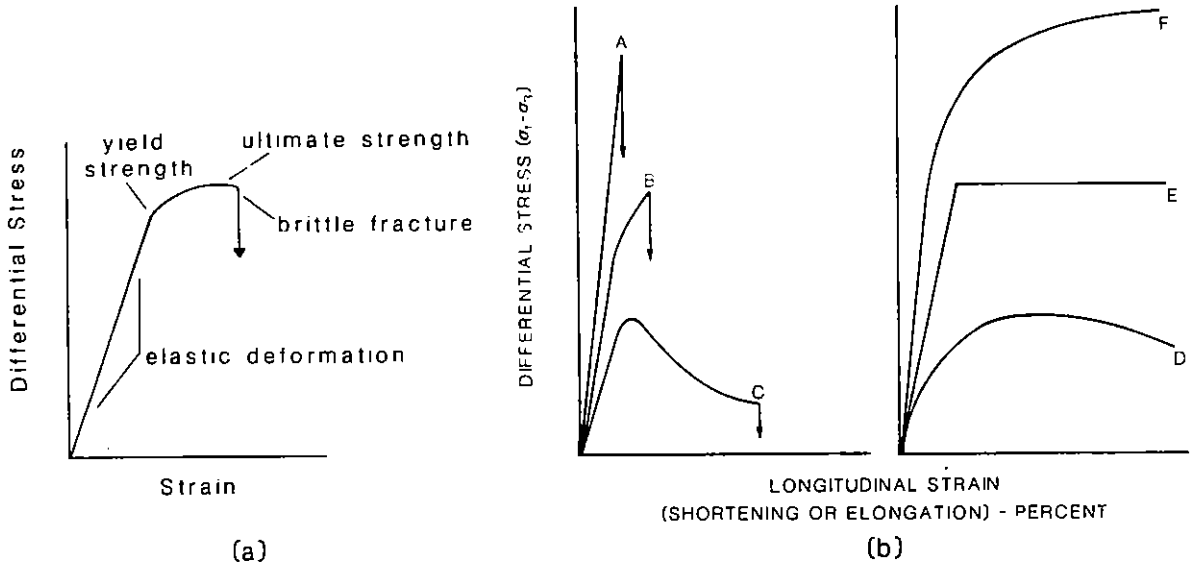

Figure 10-2. Stress-strain plots. (a) General stress-strain plot for an experiment in which a sample first deforms elastically, then yields and deforms plastically before failing. (b) Representative stress-strain plots. A = elastic deformation followed by brittle failure; note that failure is indicated by a sudden stress drop. B = elastic deformation followed by yielding, plastic deformation, then brittle failure. C = elastic deformation followed by yielding, strain softening, then brittle failure. D = strain hardening followed by strain softening. E = elastic deformation followed by yielding, then plastic deformation. F = elastic deformation followed by yielding, then strain hardening (adapted from Handin, 1966).

removed while the rock is behaving elastically, the strain returns to 0. Plastic strain is *nonrecoverable* or *permanent*, in the sense that if stress is removed after plastic strain has developed, the strain does not disappear.

A number of terms are useful in describing the behavior of a rock as displayed on a stress-strain plot. Note that in these definitions the term *strength* is measured in units of stress.

Yield strength: The value of stress ($\Delta\sigma$) at the bend in the stress-strain curve that marks the onset of permanent plastic strain.

Fracture strength: The value of stress ($\Delta\sigma$) at which a rock fails by brittle fracture. This is represented by a sudden drop in stress on the stress-strain curve.

Ultimate strength: The maximum stress ($\Delta\sigma$) that a rock sustains during an experiment (i.e., the maximum ordinate of the stress-strain curve).

Ductility: The total percent permanent strain before failure by fracture, as indicated by a marked stress drop.

The results of a constant strain-rate experiment can be be plotted not only on a stress-strain plot (Fig. 10-3a), but can also be plotted on a strain-time plot, which shows how strain changes as a function of time (Fig. 10-3b). On such a plot the horizontal axis is time, and the vertical axis is strain. Obviously, the plot for a constant strain-rate experiment must be a straight line.

The results of creep tests can be depicted by curves on a stress-strain plot (Fig. 10-3c), but the curves do not give an indication of the change in strain as a function of time. Therefore, it is often preferable to plot results of a creep test on a strain-time plot (Fig. 10-3d). The plot of results for a creep test is usually not a straight line, because the strain rate changes as strain hardening or strain softening occurs.

Representation of State of Stress on Mohr Diagrams

The stress across a specified plane can be represented by a stress vector. The *stress vector*, **P**, acting across a randomly oriented plane is inclined to the plane (Fig. 10-4) and thus can be resolved into σ_n, a *normal stress component* (perpendicular to the plane), and τ, a *shear stress component* (parallel to the plane). The state of stress at a point cannot be represented by a stress vector. Stress at a point can, however, be represented by a *stress ellipsoid*

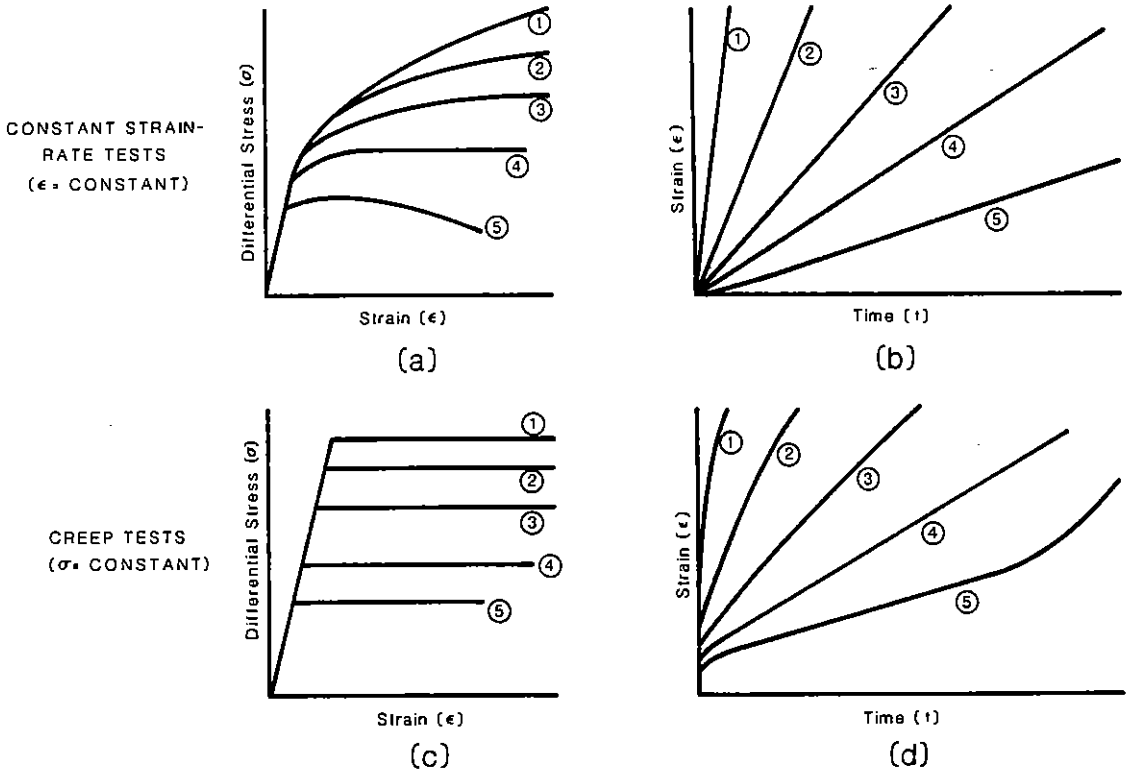

Figure 10-3. Correspondence between stress-versus-strain plots and strain-versus-time plots (adapted from Heard, 1963). (a) Stress-strain curves for constant strain-rate tests. Curve 5 is the slowest strain rate, and curve 1 is the fastest strain rate; (b) constant strain-rate experiments plotted on strain-time coordinates for the same experiments as in (a); (c) creep experiments plotted on stress-strain coordinates. Curve 1 is the fastest strain rate, and curve 5 is the slowest strain rate; (d) creep experiments plotted on strain-time coordinates for the same experiments as in (c).

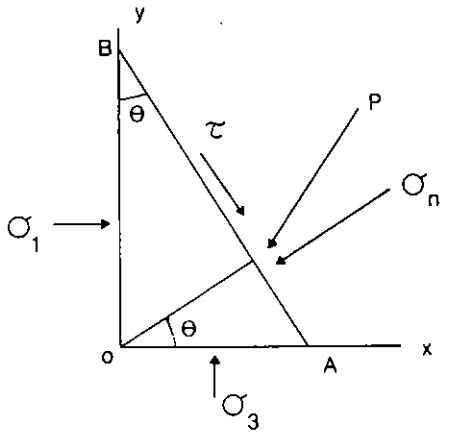

Figure 10-4. The general orientation of the principal stresses, σ_1 and σ_3, and the stress vector, **P**, resolved into σ_n and τ. The angle θ is between the normal to the plane AB and the σ_1 ('x') direction.

or a *stress tensor* (see Means, 1976, for a complete definition of these important terms). For a given stress state, there are three unique planes on which the magnitude of the shear stress component is zero. These planes are called the *principal planes*, and the stress vectors acting across them are called the *principal stresses*, where σ_1 equals the maximum principal stress at the point in question, and σ_3 equals the minimum principal stress. Principal stresses have no shear component and correspond to the principal axes of the stress ellipsoid.

If we are given the principal stresses representing the stress state at a point, we can calculate the stress vector acting across any plane of a specified orientation that passes through that point. Such calculations can be done analytically with force-balance equations or with the stress tensor (see Means, 1976, or Suppe, 1985). Fortunately, there is an easy-to-use graphic device that allows us quickly to determine the relative magnitudes of the normal and shear stress vectors in two dimensions acting across a

specified plane without going through any calculations. This device is called a *Mohr circle*. A plot containing a Mohr circle is called a *Mohr diagram*.

A Mohr circle is plotted on Cartesian axes; the x-axis represents values of normal stress (σ_n), and the y-axis represents values of shear stress (τ). The coordinates of each point on the circle represent the values of the normal and shear stress components acting across a plane of an orientation specified by the angle θ, which is measured between the pole to the plane and the maximum principal stress σ_1 (Fig. 10-4). The reason that the relative values for normal and shear stress plot along the circumference of a Mohr circle is that the circle is the locus of all points that satisfy the equations

$$\tau = {}^1/_2 (\sigma_1 - \sigma_3)\sin 2\theta \qquad \text{(Eq. 10-5)}$$

and

$$\sigma_n = {}^1/_2 (\sigma_1 + \sigma_3) + {}^1/_2 (\sigma_1 - \sigma_3)\cos 2\theta$$

(Eq. 10-6).

For a derivation of these equations using the balance of forces method, see Suppe (1985) or Means (1976).

Examination of Equations 10-5 and 10-6 indicates that the right-hand intersection of the Mohr circle with the x-axis is σ_1, and the left-hand intersection is σ_3. Therefore, to plot a circle, simply plot a point representing σ_1 and another point representing σ_3 on the x-axis (remember that principal stresses have no shear component). Place the anchor needle of a compass midway between these two points, and place the pencil of the compass on either one of the points; then simply trace out a circle with the pencil. The length of the diameter of the circle is equal to *differential stress* (σ_1-σ_3), and the x-coordinate of the center of the circle is the *mean stress* [(σ_1+σ_3)/2]. The values of σ_n and τ at a point on the circle represent the normal and shear components, respectively, of the stress vector acting on a plane oriented at and angle of 2θ measured counterclockwise from σ_1. The sign convention for Mohr diagrams used in geology is as follows: positive stresses on the x-axis are compressive, negative stresses on the x-axis are tensile, positive stresses on the y-axis represent a left-lateral shear couple, and negative stresses on the y-axis represent a right-lateral shear couple.

From the Mohr diagram the relative magnitudes of τ and σ_n on a plane inclined to the principal stresses can easily be visualized. For example, a plane inclined at 80° to σ_1 is being subjected to a greater normal stress than a plane oriented at 40° to σ_1. The plane on which shear stress is greatest is the plane oriented at 45° to σ_1.

Problem 10-1

The mean stress at a point in a rock is 40 MPa, and the differential stress is 20 MPa. (a) What are the values of σ_1 and σ_3 in the rock? (b) What are the magnitudes of τ and σ_n acting on a plane that is inclined at 30° to σ_1?

Method 10-1

Step 1: Construct coordinate axes calibrated in MPa. The horizontal axis represents σ_n, and the vertical axis represents τ (Fig. 10-5).

Step 2: Construct a Mohr circle representing the specified state of stress. The diameter of the circle is 20 MPa, and the center is positioned along the x-axis at 40 MPa. The values of σ_1 and σ_3 (Problem 10-1a) can now be read directly: σ_1 is 50 MPa, and σ_3 is 30 MPa.

Step 3: Draw a line from the center of the circle, point N, to a point, O, on the circle so that line ON makes a counterclockwise angle of 2θ (=120°) with respect to the x-axis. Remember that θ is the angle between the *normal* to the specified plane and the direction of σ_1.

Step 4: The values of τ and σ_n acting on the plane are specified by the coordinates of point O.

Representation of Failure Criteria on Mohr Diagrams

As discussed earlier, failure of a rock is manifested by a sudden stress drop. Failure under brittle conditions can be indicative of either (1) development of a new fracture surface in an intact rock or (2) slip on a preexisting fracture in a previously broken rock. A *failure criterion* is a specification of the stress state at which failure occurs. A

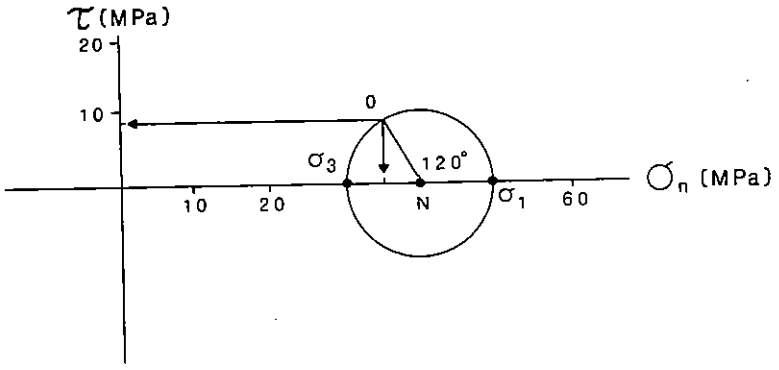

Figure 10-5. A Mohr diagram. Point N marks the value of mean stress, which is 40 MPa. $2\theta = 120°$, σ_1 = 50 MPa, σ_3 = 30 MPa. The normal stress on a plane oriented such that the angle between σ_1 and the pole to the plane is 60° is specified by the coordinates of point O.

Mohr diagram can be used to represent certain types of failure criteria. On a Mohr diagram, a failure criterion is represented by a curve that separates a field in which the state of stress is such that a rock remains stable from a field in which the state of stress is such that a rock is unstable and either ruptures or deforms by slip on a preexisting fracture. The curve is called a *failure envelope*. A failure envelope on a Mohr diagram is empirical, in that it is drawn based on laboratory experiments, not on theoretical calculations.

One of the most widely known failure criterion is the *Coulomb-Mohr failure criterion*, which is described by the equation

$$\tau = C + (\mu^*)\sigma_n \qquad \text{(Eq. 10-7).}$$

where τ is the shear stress at failure, C is a constant called the *cohesion* (the y-intercept), and μ^* is a constant called the *coefficient of internal friction* (the slope of the line). As indicated by the equation, the failure envelope defined by the Coulomb-Mohr criterion is a straight line whose slope is μ^* and whose y-intercept is the cohesion (Fig. 10-6a). The envelope cuts the abscissa at a point representing the tensile strength ($T = -\sigma_3$).

To understand what is meant by a failure envelope, consider a stress state defined by a Mohr circle that falls below the envelope and does not touch it. Such a stress state is stable, in that the rock subjected to the stress state does not fail (Fig. 10-6b). If the differential stress is increased, the diameter of the Mohr circle increases. If the differential stress is increased to a sufficiently large value, the Mohr circle becomes tangent to the envelope (Fig. 10-6c). At this instant the rock fails by formation of a fracture. If the differential stress is constant, but the mean stress decreases, the Mohr circle moves to the left along the x-axis of the Mohr diagram and eventually may touch the envelope. Again, the instant that a stress state is achieved such that the Mohr circle defining the stress state touches the envelope, the rock fails. As a consequence, it is impossible to have stress states defined by Mohr circles that extend beyond the envelope (Fig. 10-6d), because the rock will fail before such a stress state can be achieved.

Failure envelopes on a Mohr diagram are empirical, in that they are determined experimentally rather than by means of theoretical calculations. In the experiment described next, we see how a failure envelope is determined. You will find that real envelopes are not always perfectly straight lines.

10-3 ANALYSIS OF ROCK STRENGTH AND FAILURE CRITERIA

The study of rock strength at elevated temperature and pressure was greatly advanced in the 1950s by John Handin and his colleagues at the Shell Development Company.

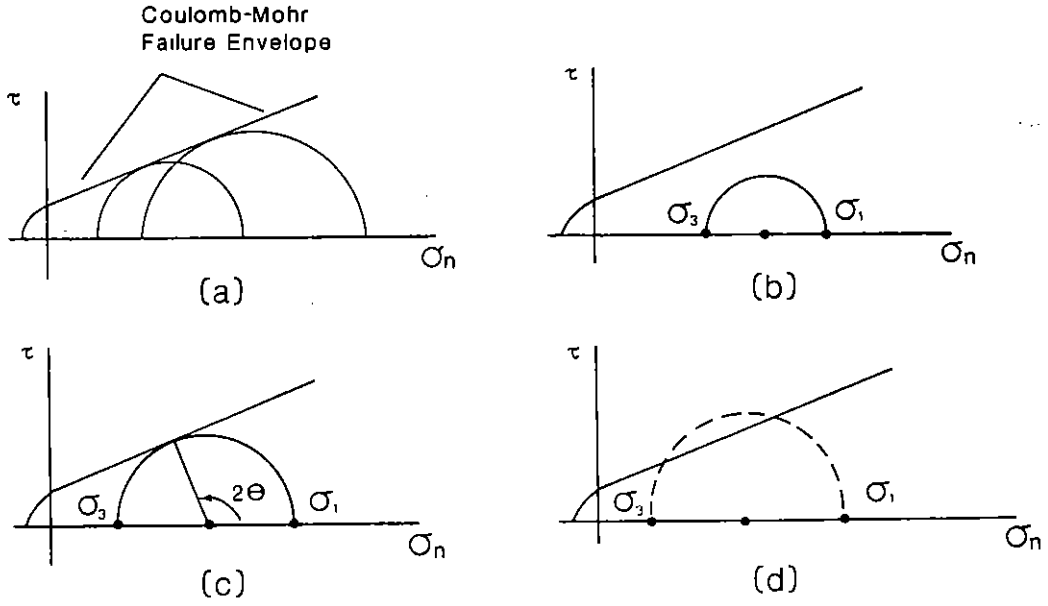

Figure 10-6. Coulomb-Mohr failure envelope. (a) Failure envelope showing the position of the y-intercept; (b) Mohr circle that is not tangent to the failure envelope and therefore represents a stable stress state; (c) Mohr circle that is tangent to the envelope and represents the stress state at the instant of failure; (d) Mohr circle representing an unstable and impossible stress state.

Handin's group systematically characterized the brittle strength of various types of rock (e.g., Handin and Hager, 1957). Experiment 1 shows how results obtained at the Shell Lab during this period can be used to determine a failure envelope for a brittle rock.

Determination of the Failure Envelope for Brittle Fracture

Experiment 10-1 (Oil Creek Sandstone)

The purpose of this experiment was to determine the failure envelope that characterizes the strength of Oil Creek Sandstone (a massive, very fine-grained, well-sorted, well-cemented Ordovician sandstone from Grayson County, Texas). To obtain each experimental data point a jacketed cylinder of sandstone was placed in a triaxial rock-deformation machine. Then the confining pressure was set at a specified value, and the axial stress (σ_1) was increased until the specimen failed. Note that by increasing the value of σ_1 while σ_3 was held constant, we increased the differential stress. This increase was represented by an increase in the diameter of the Mohr circle defining the stress state in the sample. Individual experiments differed from one another in the value of the confining pressure (σ_3) set at the beginning of the experiment. All experiments were carried out at room temperature and at a strain rate of about 10^{-3} per second.

Results 10-1

The raw data of each experiment (run) were replotted on a graph in which the x-axis was axial strain and the y-axis was differential stress. In each case, when the sample achieved its ultimate strength, it failed brittlely by formation of a discrete shear fracture. In Figure 10-7 three stress-strain curves obtained during the experiment are shown (from Handin and Hager, 1957). The confining pressure for each run is indicated on the graph. The strength of the sample under the specified confining pressure is the maximum stress achieved before the sudden stress drop occurred. The stress drop is indicated by the small arrow at the end of the curve. Figure 10-8 provides a sketch of a ruptured specimen after completion of the experiment, showing the orientation of the shear fracture (the measured $\theta = 67^{\circ}$).

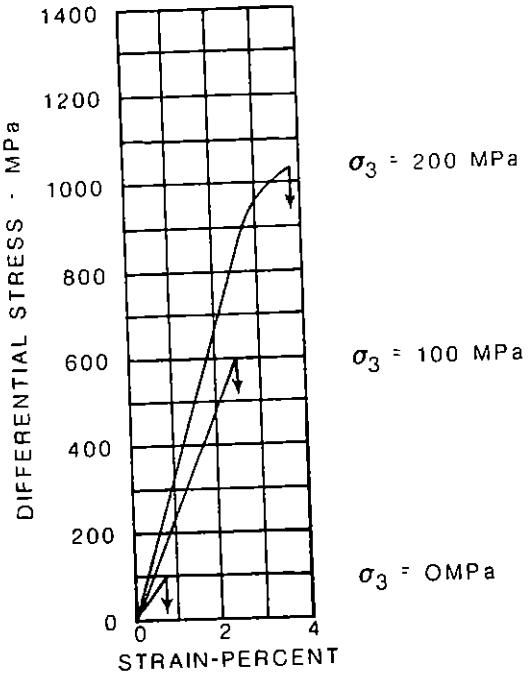

Figure 10-7. Stress-strain curves for Oil Creek Sandstone (adapted from Handin and Hager, 1957). The confining pressure is indicated next to the curve.

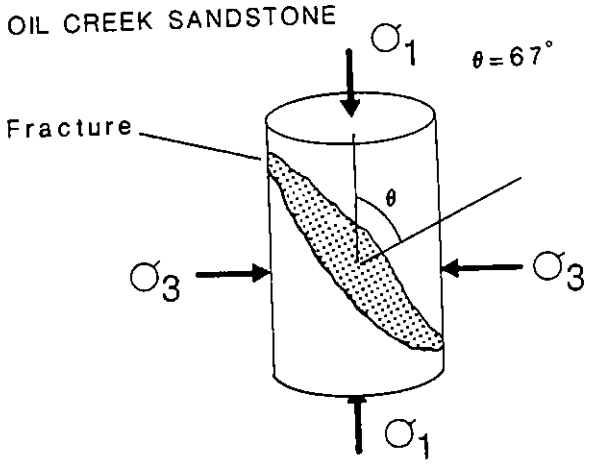

Figure 10-8. A drawing of fractured Oil Creek Sandstone. The stippled plane is the fracture surface.

Interpretation 10-1 (to be completed by the student)

(a) Using the stress-strain plots of Figure 10-7, determine the differential stress and the mean stress at the point of brittle fracture for each run.

(b) Draw the coordinate axes of a Mohr diagram at an appropriate scale. On the diagram draw the Mohr circle showing the stress state at failure for each run (i.e., you should draw three nonconcentric circles centered at the mean stress for the respective experiment). Note that you must first calculate σ_1 from knowledge of the differential stress and σ_3.

(c) Draw the two curves that are tangent to all three circles. One curve will lie above the x-axis, and one curve will lie below the x-axis. These curves define the failure envelope. Are the curves straight or bent?

(d) Calculate the equation that approximately describes the curve that lies above the x-axis (i.e.,

determine appropriate values for the constants in Equation 10-7). This equation is the Coulomb-Mohr failure criterion for Oil Creek Sandstone.

(e) The orientation of the failure plane is determined by the obtuse angle between the x-axis and the line connecting the center of a particular circle and the point of tangency with the envelope. Is the orientation of the failure plane indicated by each circle the same?

(f) Is the orientation of the observed fracture plane the same as the fracture orientation suggested by the Coulomb-Mohr failure criterion?

(g) How does confining pressure affect the fracture strength of Oil Creek Sandstone?

(h) From your answers to parts a-f, complete Table 10-1. Write a paragraph outlining the conclusions that can be drawn from the experiments on Oil Creek Sandstone. In particular, suggest what applications the results might have toward predicting the stability of boreholes?

Study of the Brittle-Ductile Transition

Experiment 10-2 (Berea Sandstone)

Handin et al. (1963) conducted a set of experiments on Berea Sandstone (medium-grained, poorly cemented Mississippian sandstone from Ohio), using the procedures outlined in Experiment 10-1. The Berea Sandstone is weaker than the Oil Creek Sandstone. In these experiments the specimens contained pore fluid under pressure. Handin et al. ran five experiments. In each experiment, the confining pressure was the same (200 MPa), but the pore pressure varied (0, 50, 100, 150, and 200 MPa, respectively). The purpose of these experiments was to determine the failure envelope that characterized the strength of Berea Sandstone under conditions of elevated pore pressure. (The data used here have been modified slightly from the original experiments in order to make the results more obvious.)

Results 10-2

Figure 10-9 provides the stress-strain plots for five runs (adapted from Handin et al., 1963). The effective confining pressure associated with each curve is indicated next to the curve. It is evident from the curves in Figure 10-9 that Berea Sandstone does not lose complete strength after yielding; there was not a sudden loss of cohesion accompanied by a catastrophic stress drop, as was the case for the Oil Creek Sandstone. At higher confining pressures it was observed that the sandstone specimens continued to strain without a stress drop even after fractures had developed. Note that the ultimate strength continued to increase with increasing confining pressure.

Table 10-1
Oil Creek Sandstone

Run number	Confining pressure	Differential stress at failure	σ_1 at failure	Fracture angle
1				
2				
3				

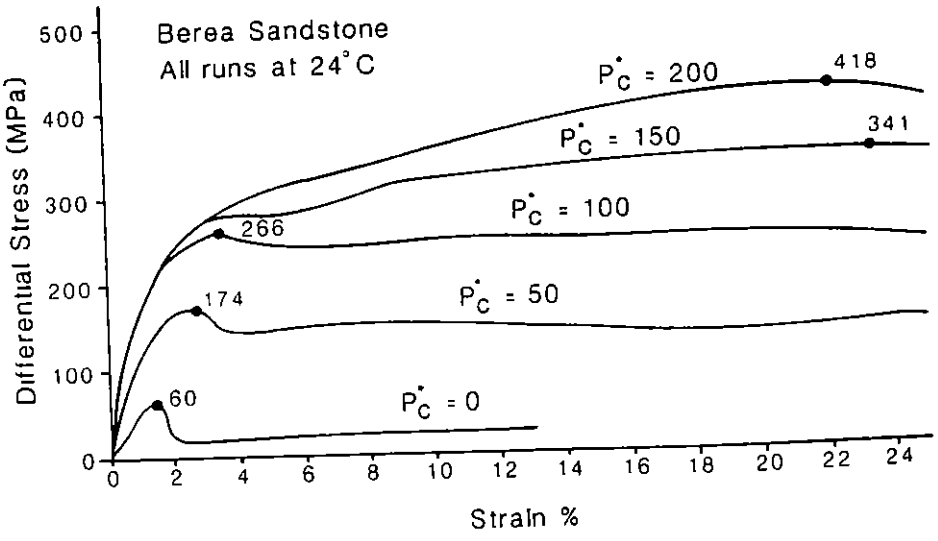

Figure 10-9. Stress-strain curves for Berea Sandstone (adapted from Handin et al., 1963). P_C^*, the effective confining pressure, for each run is indicated next to the curve. The value of differential stress at the ultimate strength is also indicated.

Interpretation 10-2 (to be completed by the student)

(a) Look at the curves shown in Figure 10-9. Note that the curves for runs at lower effective confining pressure are different in shape from the curves at higher effective confining pressure. Describe the difference in curve shape. (*Hint:* Compare these curves with those shown in Figs. 10-2 and 10-3a. Explain how the series of curves in Figure 10-9 shows the transition from brittle behavior to ductile behavior). Is the yield strength the same as ultimate strength for all curves? Under what conditions does strain hardening occur?

(b) After examining Figure 10-9, indicate how the strain (in percent) at which ultimate strength is reached is related to effective confining pressure. Remembering the definition of ductility (ductility = total percent strain before fracture), explain how ductility is related to effective confining pressure.

(c) Construct a Mohr diagram, and plot the Mohr circle corresponding to each experiment. Use the ultimate strength to define the differential stress at failure, and consider the effective confining pressure to be σ_3. Draw the failure envelope so that it is tangent to each circle. How does the failure envelope constructed from this experiment differ from that constructed in Experiment 10-1 for Oil Creek Sandstone?

(d) From the Mohr diagram, determine how the fracture angle changes as a function of confining pressure. Is there a systematic change? Try to explain why this change occurs. The measured fracture angles (angle between σ_1 and the plane of the fracture) were 26° at 0 MPa, 27° at 50 MPa, 34° at 100 MPa, 36° at 150 MPa, and 38° at 200 MPa confining pressure, respectively. Note that these angles are somewhat different from those derived from the Mohr diagram, probably reflecting the qualitative nature of the Coulomb-Mohr failure envelope.

(e) Based on the observations in this experiment, do you estimate that wet Berea Sandstone subjected to the stress conditions at a depth of 1 km in the earth will lose strength by brittle fracture or maintain strength by ductile-like behavior? What about dry Oil Creek Sandstone? Assume that differential stress in the upper crust is $2/3(\rho gh)$, where ρ is the average density of rock (2.7 g/cm^3), g is the gravitational constant (980 cm/s^2), and h is the depth measured in centimeters. Means (1976) explains why the differential stress in the upper crust is approximately $2/3(\rho gh)$.

(f) Note that in this experiment we have used the term "effective" confining pressure to emphasize that the samples contained pore fluid under pressure. Will a change in the pore pressure affect the equation of the failure envelope for a given rock?

(g) The confining pressure on a sample of Berea Sandstone is set at 100 MPa, and the axial stress is set at 210 MPa. Based on the failure envelope you determined above, will the sample fail if the pore pressure is 50 MPa? Will a sample fail if the pore pressure is 60 MPa? How does an increase in the pore pressure of 75 MPa affect the position of the Mohr circle? How does an increase in pore pressure of 60 MPa affect the values of mean stress and differential stress?

10-4 ANALYSIS OF DUCTILE DEFORMATION

During brittle deformation only a small elastic strain (< 3%) is achieved before failure occurs by formation of a brittle fracture. During *ductile deformation* of rock, fracture does not occur even after large strain is achieved (> 25%). In other words, during ductile deformation large strains develop without loss of cohesion. Rock that fails by brittle fracture when the strain is between 3% and 25% is said to exhibit brittle-ductile behavior. We observed the transition from brittle to ductile behavior in the experiment on Berea Sandstone. It is obvious that ductile deformation is common in nature, for there are many geologic settings in which folding occurs, without the aid of brittle fracture. Next, we consider triaxial loading experiments in which environmental conditions are manipulated so that ductile deformation can occur.

Experiment 10-3 (Solenhofen Limestone, Carrara Marble, Yule Marble)

The three environmental parameters that are most important in determining whether rock behaves brittlely or ductilely are temperature, confining pressure, and strain rate. Heard (1960) and Edmond and Paterson (1972), among others, have examined how these variables affect the ductility of rock. In the experiments a cylinder of rock was placed in a triaxial loading machine. Confining pressure was exerted by increasing the pressure of argon in the pressure chamber, and temperature was increased by an electrical furnace. The strain rate was varied by changing the rate at which the piston moved. In some experiments the sample was stretched rather than shortened. We describe four sets of experiments.

(a) Variable Confining Pressure: Edmond and Paterson (1972) deformed cylinders of Carrara Marble at room temperature and at a strain rate of 4×10^{-4} s^{-1} They repeated the experiment six times, each time with a new rock cylinder and under a different confining pressure. Differential stress versus axial strain curves for the experiments are shown in Figure 10-10a.

(b) Variable Confining Pressure: Heard (1960) deformed cylinders of Solenhofen Limestone under compression at room temperature. He repeated the experiment seven times, each time at a different confining

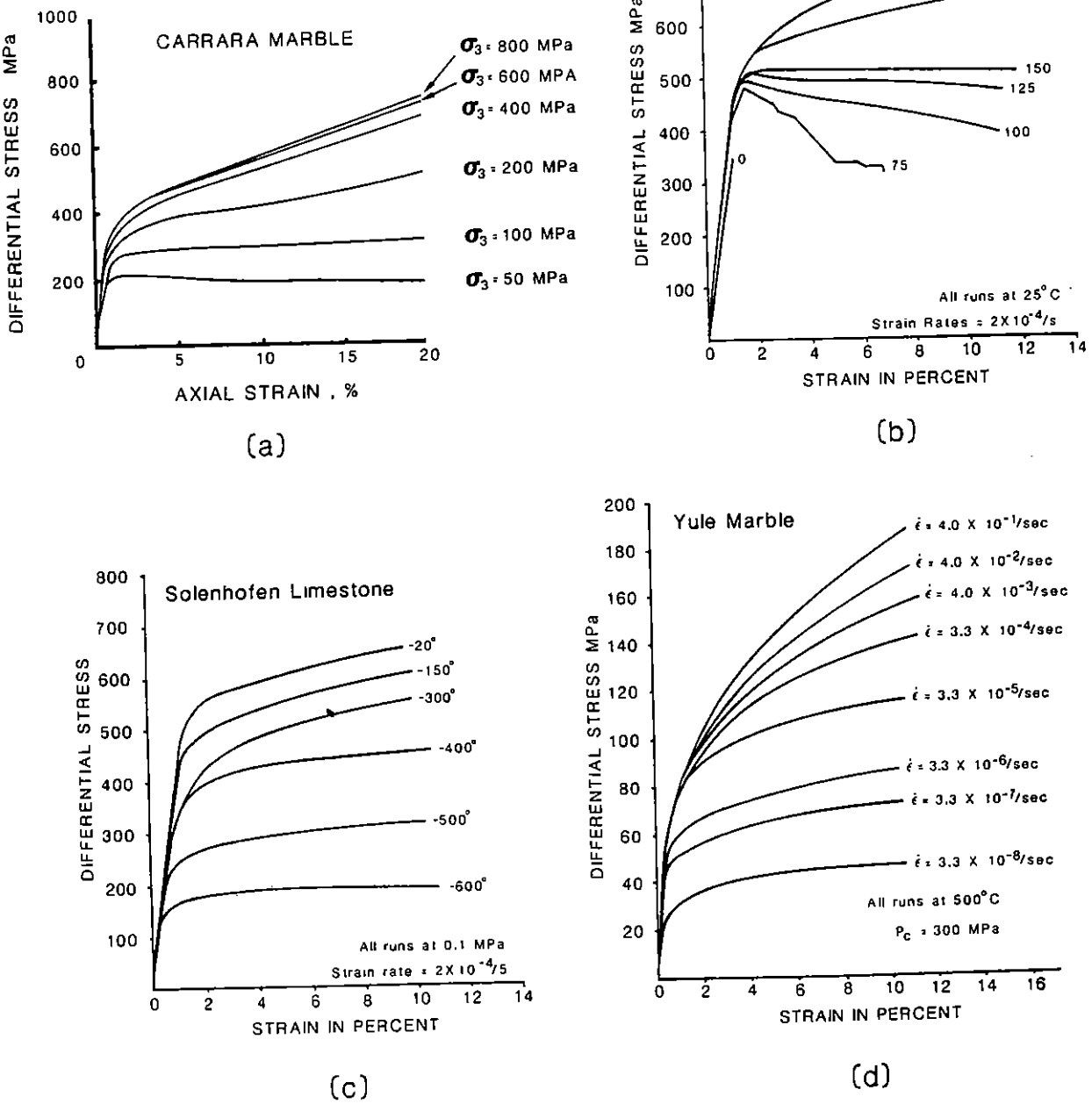

Figure 10-10. Effect of environment on ductile behavior. (a) Differential stress versus axial strain for triaxial compression tests on Carrara Marble under variable conditions of confining pressure (adapted from Edmond and Paterson, 1972); (b) differential stress versus axial strain for triaxial compression tests on Solenhofen Limestone under variable conditions of confining pressure at a constant strain rate (adapted from Heard, 1960); (c) differential stress versus axial strain for triaxial compression tests of Solenhofen Limestone under variable conditions of temperature (adapted from Heard, 1960); (d) differential stress versus strain for triaxial extension tests on Yule Marble at 500°C and 500 MPa (adapted from Heard, 1963).

pressure. The results of the experiments and the confining pressures are indicated on Figure 10-10b.

(c) Variable Temperature: Heard (1960) deformed cylinders of Solenhofen Limestone under compression at a strain rate of 2×10^{-4} s^{-1} and a confining pressure of 300 MPa. He repeated the experiment six times, each time with a new rock cylinder. The results and the temperatures are indicated in Figure 10-10c.

(d) Variable Strain Rate: Heard (1963) deformed Yule Marble by extension at a temperature of 500°C. He repeated the experiment eight times, each time with a new rock cylinder and at a different strain rate. The results and the strain rates are indicated in Figure 10-10d.

Interpretation 10-3 (to be completed by the student)

(a) For each set of experiments describe how the yield strength varies as a function of the environmental condition. To emphasize your result make a plot of yield strength (in terms of differential stress) as a function of the environmental parameter (i.e., confining pressure, temperature, strain rate).

(b) Considering the results of these experiments, provide generalizations concerning the relationship of ductility to deformational environment. Under what conditions will ductile deformation be more likely?

(c) Compare the results of the variable confining pressure experiments for Solenhofen Limestone (Experiment 10-3b) with those of the experiments for Carrara Marble (Experiment 10-3a). Solenhofen Limestone is a very fine grained carbonate, whereas Carrara Marble is a relatively coarse grained carbonate. Is there a dependence of ductility on grain size?

(d) Carbonates are relatively ductile compared to granite. What types of stress-strain curves would you expect for granite under the conditions of Experiments 10-3a and 10-3b? (*Hint:* Look again at the stress-strain plot for Oil Creek Sandstone, and remember that some sandstones, like granite, are stronger than carbonates).

(e) Considering the state of stress in the crust, at what depth would you expect ductile behavior to become dominant over brittle behavior (the *brittle-ductile transition*) for Solenhofen Limestone, assuming that temperature does not change with depth? Assume that differential stress in the upper crust is $2/3(\rho g h)$, where ρ is the average density of rock (2.7 g/cm^3), g is the gravitational constant (980 cm/s^2), and h is the depth measured in centimeters.

(f) In reality the geothermal gradient in the crust is about 30°C/km (i.e., at 1-km depth, the temperature is 30°C greater than at the surface). Keeping this in mind, at approximately what depth would you expect the brittle-ductile transition for Yule Marble to occur, neglecting the effect of confining pressure?

(g) Folds, which are manifestations of ductile deformation, are known to develop in the upper crust above the brittle-ductile transition. Furthermore, in many deformational settings, folding and brittle faulting occur during the same period of time. Considering the results of the experiments described above, explain this paradox.

10-5 ANALYSIS OF ROCK FRICTION

Experiments 10-1 and 10-2 concerned the initiation of a fracture in an intact rock. Once a rock contain fractures, deformation may continue by additional slip on these fractures. *Friction* is the resistance to sliding on a fracture surface. To initiate sliding on a surface, the component of shear stress parallel to the surface must exceed a critical value called the *frictional strength.* In general, frictional strength depends on the magnitude of normal stress across the surface; as the normal stress increases, it becomes progressively harder for sliding to take place, and thus the shear stress necessary to initiate sliding must increase. The *coefficient of friction* (μ) is the ratio between the shear stress necessary to initiate sliding and the normal stress across the surface:

$$\mu = \tau/\sigma_n \qquad \text{(Eq. 10-8).}$$

The value of μ can be determined from a single experiment in which the value of τ at a given σ_n is measured. Experimental work suggests that μ is not constant but depends on the value of σ_n. If a series of tests is conducted, each at a different σ_n, and the results are plotted using Cartesian axes (x-axis is σ_n, and y-axis is τ), we can define another coefficient of friction (μ'), which is the slope of the line passing through the data points. This line is a failure envelope that may be used in the same manner as the Coulomb-Mohr envelope to predict frictional sliding on favorably oriented fractures. For measurements made under high pressure, the sloping line intercepts the τ-axis above zero. Therefore, the equation of the line is

$$\tau = S_0 + \mu'\sigma_n \qquad \text{(Eq. 10-9),}$$

where S_0 is the intercept between the friction envelope and the τ-axis. S_0 represents the shear stress necessary to initiate sliding under conditions such that σ_n is 0 (i.e., it is the cohesive strength of the fracture). We can solve for μ' and derive the equation

$$\mu' = (\tau - S_0)/\sigma_n \qquad \text{(Eq. 10-10).}$$

The coefficient of friction (μ') can also be defined in terms of the angle (ϕ) between the friction envelope and the horizontal. This angle is called the *angle of friction*, and

$$\mu' = \tan \phi \qquad \text{(Eq. 10-11).}$$

In the following experiments, we see how to determine the value of μ'.

Analysis of Failure Envelopes for Frictional Sliding

Experiment 10-4 (Tennessee Sandstone)

John Handin at Shell Development Company measured the frictional properties of Tennessee Sandstone. For each experimental run he used a 1.9 x 5.0 cm cylinder of sandstone containing one through-going saw cut inclined at 45° to the cylinder axis. Each saw-cut surface was polished to allow a good fit when mated to reform a cylinder. The samples were jacketed in lead and placed in a triaxial rock deformation machine. The stress at which sliding occurred (i.e., the *frictional strength*) was measured by subjecting the specimen to an axial load and observing when a displacement occurred on the saw-cut surface. The experiment was repeated for a range of confining pressures as listed in Table 10-2.

Results 10-4

Table 10-2 lists the μ (the ratio of τ/σ_n) for individual experiments (Handin, 1969). Note that the normal and shear stress terms were calculated by resolving the axial stress on a plane oriented at 45° to the axial stress. All stresses were measured in MPa. Note that the coefficient of friction is dimensionless.

Interpretation 10-4 (to be completed by student)

(a) Derive μ' based on the slope of the line of τ versus σ_n.

(b) Write the general equation for the frictional sliding of Tennessee Sandstone. Note that μ' in this equation is by definition independent of confining pressure.

(c) How does the coefficient of friction (μ) for individual tests depend on confining pressure? This relationship is best illustrated by plotting a graph of μ against confining pressure.

Determination of the Preference for Fracture over Frictional Sliding

Experiment 10-5 (Blair Dolomite, Solenhofen Limestone, Leuders Limestone, Tennessee Sandstone)

The shear stress necessary to initiate sliding on a preexisting fracture depends on the normal stress across the fracture, as can be illustrated by comparing shear stress and normal stress in Table 10-2. The normal stress across a fracture plane depends on its orientation relative to σ_1. If a fracture is oriented such that the normal stress across the fracture is high (i.e., 2θ is small), the rock may fail by formation of a new fracture before the preexisting fracture can slip. It is possible to determine conditions under which frictional sliding precedes fracture for a given rock by comparing the envelope for frictional sliding with the Coulomb-Mohr failure envelope.

Handin (1969) described a series of experiments designed to investigate the preference for new fracturing before slip on preexisting rock fractures. He obtained 1.9 X 5.0-cm cylinders of several rock types (Blair Dolomite, Solenhofen Limestone, Leuders Limestone, and Tennessee Sandstone) and made a cut at a specified angle in each sample. These cuts represented preexisting fractures in the test samples. The opposing surfaces of each cut were lightly polished so that they closed tightly. The samples were jacketed in lead and placed in a triaxial rock-deformation machine. The stress at which sliding occurred (i.e., the *frictional strength*) was measured by subjecting the specimen to an axial load and observing when a displacement occurred on the fracture. The

Table 10-2
The Frictional Properties of Tennessee Sandstone

Confining pressure	Shear stress τ	Normal stress σ_n	Coefficient of friction μ
25	76	100	0.76
50	130	180	0.72
75	181	255	0.71
100	231	330	0.70
125	287	410	0.70
150	331	480	0.69
175	386	560	0.69
200	420	620	0.68

experiments were repeated for the same rock type, for different fracture orientations in each rock type, and for a range of confining pressures.

Results 10-5

The results of the work on preference for fracturing or sliding are presented in the form of fracture and friction envelopes in Table 10-3. In some specimens deformation was accommodated entirely by movement on the preexisting fracture, in some specimens deformation was accommodated by formation of a new fracture in addition to sliding on a preexisting fracture, and in some specimens deformation was accommodated only by initiation of a new fracture (Fig. 10-11).

Interpretation 10-5 (to be completed by student)

(a) On a Mohr diagram construct both the Coulomb-Mohr failure envelope and the sliding friction envelope for the four lithologies listed in Table 10-3. Note that the saw cuts are cohesionless, so the frictional failure line passes through the origin.

(b) For the runs identified in Table 10-3 compare the coefficients of sliding friction and the coefficients of internal friction. Consider an experiment in which the confining pressure is 100 MPa, and the differential stress is gradually increased. From the data in Table 10-3 determine whether any of the rocks will fail first by slip on a preexisting fracture inclined at 45° to the axial load or whether they will fail by formation of a new fracture.

(c) Consider an experiment run at a mean stress of 400 MPa. For Tennessee Sandstone what are the angles of the preexisting fracture for which new fracture will take place while the preexisting fracture remains stable (i.e., does not slide)?

(d) The crust of the Earth contains fractures in many orientations. Using your answers to the preceding questions, and Tables 10-2 and 10-3, explain why differential stress magnitude in the upper crust is controlled by frictional sliding criteria rather than by failure criteria.

(e) If the axial stress is 207.6 MPa and the confining pressure is 92.4 MPa, determine the shear stress on each of the two planes shown in the cylinder of rock (Fig. 10-12) used for a deformation experiment. Assuming that both discontinuities exist within the rock cylinder, on which plane will frictional slip be favored? (Draw the Mohr diagram very carefully.)

Table 10-3
Faulting and Friction Envelopes

Rock type	Coulomb-Mohr envelope	Friction envelope
Blair Dolomite	$\tau = 45 + \sigma_n \tan 45°$	$\tau = \sigma_n \tan 21°$
Tennessee Sandstone	$\tau = 50 + \sigma_n \tan 40°$	$\tau = \sigma_n \tan 35°$
Solenhofen Limestone	$\tau = 105 + \sigma_n \tan 28°$	$\tau = \sigma_n \tan 32°$
Leuders Limestone	$\tau = 15 + \sigma_n \tan 28°$	$\tau = \sigma_n \tan 31°$

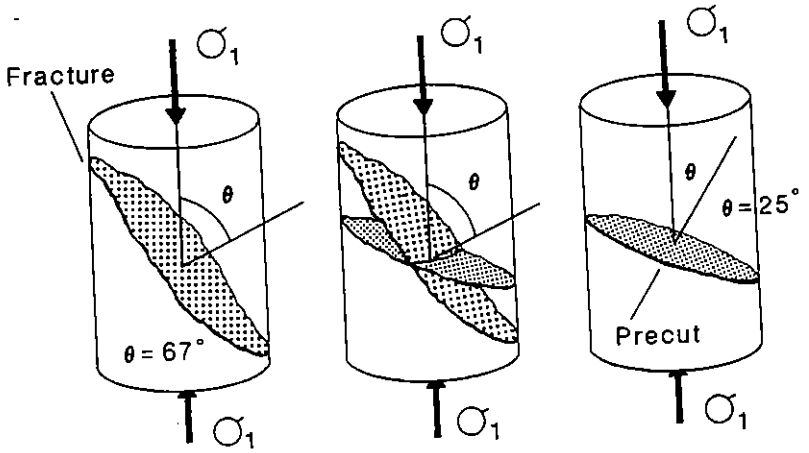

Figure 10-11. Three samples of Blair Dolomite: one with a fracture; one with a saw cut, and one with both. The lightly stippled plane is a fracture that formed in intact rock. The darker shaded plane is a saw cut.

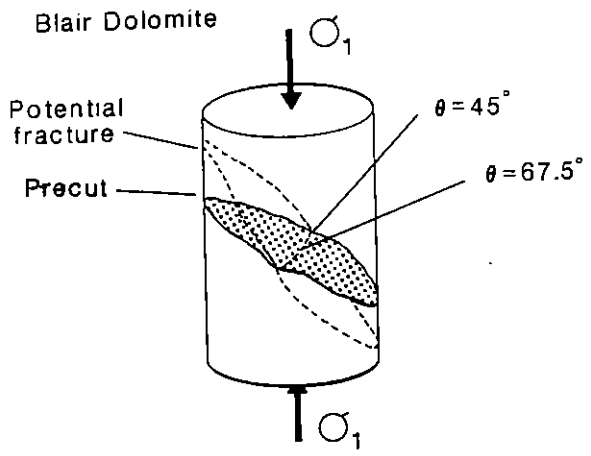

Figure 10-12. A cylinder of Blair Dolomite with two fracture surfaces (for Experiment 10-5).

Friction and an Explanation for Stress in the Earth's Crust

In the late 1970s a large number of *in situ* stress measurements were made in outcrops, drill holes, and mines. Comparison of the results from in situ measurements with laboratory measurements indicated that ambient stresses in the upper crust of the earth are generally too low to initiate fractures in intact rock. It was suggested that the relatively low ambient stress state of the earth's upper crust did not, therefore, reflect the strength of intact rock but rather reflected the magnitude of shear stress necessary to cause sliding on preexisting fractures. The crust is pervaded with joints and fractures; it is intuitively reasonable to assume that slip will occur on one of these fractures long before the magnitude of differential stress becomes high enough to cause rupture of intact rock between the fractures. In order to better understand stresses in the earth's upper crust it is therefore necessary to understand the conditions under which sliding along natural fractures can initiate.

The data for Tennessee Sandstone from Table 10-2 are plotted on a Mohr diagram (Fig. 10-13). This is the answer to a question in Experiment 10-5. To a first approximation these data appear to follow a linear trend defining a Mohr-like envelope called the *friction envelope.* Byerlee (1978) compiled a large quantity of friction data for a great variety of rock types. After plotting his data in the same format as that of Figure 10-13, Byerlee (1978) observed that most of the friction data for rocks followed a general trend divided into two linear segments. Those data for experiments with a mean stress of less than 200 MPa followed the friction equation

$$\tau = 0.85(\sigma_n) \qquad \text{(Eq. 10-12),}$$

whereas data from experiments with mean stress > 200 Mpa followed the friction equation:

$$\tau = 50 + 0.6(\sigma_n) \qquad \text{(Eq. 10-13).}$$

Experiment 10-6 (Barre Granite)

In this experiment we wish to demonstrate that Coulomb-Mohr analysis can be used to determine which fracture orientation is most favorable for slip. To do so, we create an experimental rock cylinder of Barre Granite with three fractures (saw cuts that have been slightly polished) as shown in Figure 10-14. Normals to the fractures make angles of 45°, 60°, and 75° to σ_1, respectively. We place the rock in a triaxial load machine, set the confining pressure at 150 MPa, and gradually increase the axial load until failure by sliding on a fracture occurs.

Results 10-6

The granite sample fails by sliding on one of the fractures when the value of σ_1 reaches a sufficiently high

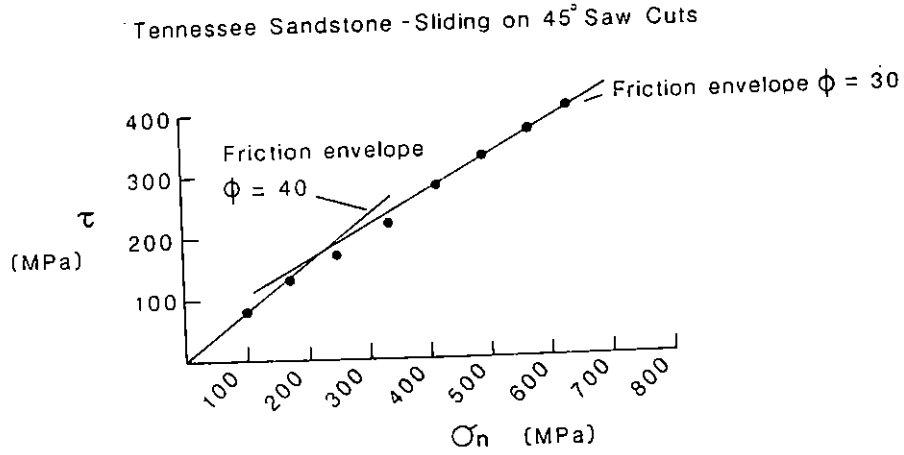

Figure 10-13. Mohr diagram for frictional sliding of Tennessee Sandstone.

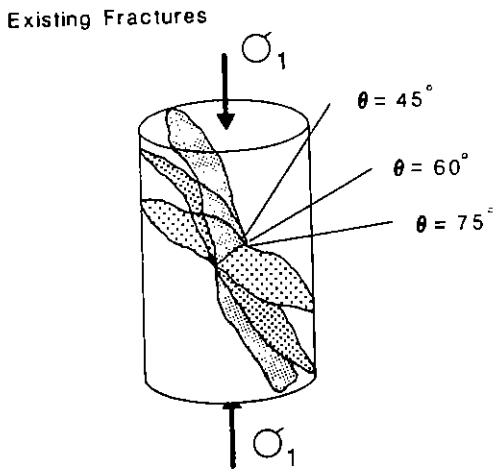

Figure 10-14. Three preexisting fractures in a cylinder of Barre Granite (for Experiment 10-6). The angle θ is the angle between the pole to the fracture and the σ_1 direction. The fractures all intersect along a line that is perpendicular to the cylinder axis.

value. Because the sample is jacketed, we cannot determine which fracture slipped until we remove the sample from the machine and strip off its jacket. In order to prove that the Coulomb-Mohr analysis correctly predicts the orientation of the slipped fracture, we first complete the following steps of interpretation (i.e., predict the differential stress at failure and predict which fracture failed first).

Interpretation 10-6

(a) First, we attempt to predict the differential stress at the time of failure. We know that σ_3 is 150 MPa, so we guess that the mean stress is at least 300 MPa. If this guess is correct, we can use the general friction equation (Eq. 10-13) to define the failure envelope for frictional sliding. We construct a Mohr diagram showing this frictional sliding envelope. The friction equation states that the coefficient of friction is 0.60, that the frictional sliding envelope has a slope of 31°, and that the rock behaves as if it has a "cohesive strength" of about 50 MPa.

(b) We plot the specified σ_3 on the x-axis. We know that the rock failed by sliding, so by trial and error we use a compass to find the Mohr circle that passes through the 150-MPa mark and is tangent to the failure envelope. Then, with a compass, we draw a circle centered at this point and tangent to the sliding envelope. Now that we have the Mohr circle, we determine the mean stress and the differential stress at the time of failure. Considering the mean stress that we determined, was it reasonable to use Equation 10-13 rather than Equation 10-12 to specify the failure envelope?

(c) We draw a line from the center of the Mohr circle to the point of tangency between the circle and the failure envelope and measure the angle 2θ. Given this angle, we can determine the orientation of the fracture that probably slid first. What is it? Note that this plane is not the plane on which shear stress was greatest. Why did it slide first? Why do you expect the other fractures to be stable under these stress conditions?

(d) Consider a hypothetical state of stress in the upper crust of the earth. Vertical stress is σ_1 and is due to the weight of overlying rock. The magnitude of σ_1 is ρgh. In the absence of tectonic stress, horizontal stress in the upper elastic crust is due to lateral expansion of the rock in response to the vertical load. Assume the value of horizontal stress to be $\sigma_2 = \sigma_3 = {}^1/_3(\rho gh)$. Determine the mean stress, differential stress, and depth in the crust at which $\sigma_2 = \sigma_3 = 150$ MPa ($\rho = 2.7$ g/cm^3, and $g = 9.8$ m/s^2). Assuming that the predictions made above are correct, how do these stresses compare with the stresses at the time of failure in the experiment? Do you expect that at a depth of 10 km in the earth that one or both fracture sets will slide in dry rock ? If not, by how much can pore fluid pressure increase before slip on a fracture set will occur.

A Mohr diagram constructed from the data in Table 10-3 for Blair Dolomite is shown in Figure 10-15a. In this diagram the Mohr circle represents the stress state at which a shear fracture develops under a confining pressure of 100 MPa. The Coulomb-Mohr failure envelope is tangent to the Mohr circle at Point O. The radius ON makes a 2θ angle of 135° measured counterclockwise from the x-axis. Therefore, the Mohr diagram indicates that a fracture developed in intact rock that fails under a confining pressure of 100 MPa should be oriented at an angle of 22.5° to σ_1.

Using data from Handin's friction experiments (described above), we find that the friction envelope for Blair Dolomite has a relatively shallow slope (θ = 21°). This envelope is not the same as that specified by Equation 10-12 and, therefore, does not fit the general friction equations given above. This discrepancy may be a consequence of the experimental conditions used by Handin. In his experiments the saw cuts were quite smooth, so there may have been little interlocking across the saw cut; therefore, resistance to shear was less than expected.

Examination of Figure 10-15a allows us to predict the range of possible orientations for which slip on a preexisting fracture is favored over fracture through intact Blair Dolomite. To do this, we locate the intersections between the envelope for frictional sliding and the Mohr circle and label the two points of intersection A and B. Then we draw the two radii of the Mohr circle that

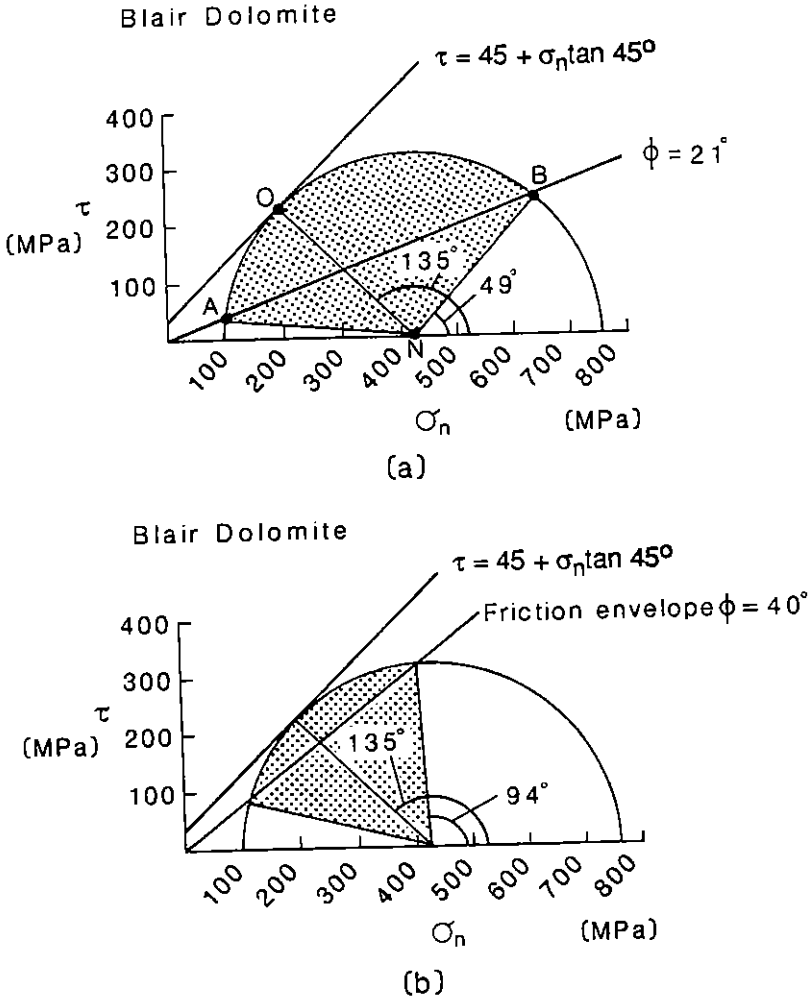

Figure 10-15. Mohr diagrams for Blair Dolomite. Only fractures represented by lines that fall in the stippled intervals on the diagrams can slip. If there are no favorably oriented fractures in the rock, then the rock fails when the circle touches the Coulomb-Mohr envelope. (a) Diagram showing both the Coulomb-Mohr failure envelope and the envelope for frictional sliding determined by Handin (1969); (b) diagram showing both the Coulomb-Mohr failure envelope and the general envelope for frictional sliding proposed by Byerlee (1978).

terminate at A and B. These radii are lines NA and NB. The wedge of the circle that lies between NA and NB (shaded in Fig. 10-15a) represents the range of 2θ values for which slip on a preexisting fracture will occur at stresses lower than those necessary to cause a new fracture to form. If we had used the general friction equations to represent the frictional strength of Blair Dolomite, then a smaller range of fracture orientations would favor slip over fracture initiation. Figure 10-15b shows that if the general friction equations are applied to Blair Dolomite, an existing fracture inclined at 45° to σ_1 is not favored over development of a new fracture at 22.5° to σ_1. However, a fracture inclined at 43° to σ_1 is equally likely to slip as a new fracture is to form.

10-6 FRICTIONAL PROPERTIES OF FAULT GOUGE

So far the frictional properties of fractures and joints have been examined by using experiments where intact rock is sliding on intact rock. If slip continues on these breaks in rock, a layer of fault gouge will build up by the grinding and milling of the rock in contact with the slip surface. Before much slip the fracture will become a fault zone with a layer of fault gouge between intact rock. The gouge will act to change the frictional properties of the rock depending on the strength of the fault gouge. The effect of gouge on the frictional properties of rock has been investigated in the laboratory.

Experiment 10-7 (quartz gouge and halite gouge)

Many real faults are not planes along which two clean rock surfaces are juxtaposed. During faulting, fault gouge composed of finely ground rock, may accumulate along the fault. In some circumstances, a particularly ductile material, such as halite, may occur along a fault. Halite can be incorporated along faults that pass through evaporite sequences. In such circumstances the frictional strength of the fault is affected. A number of experiments have been conducted to study how the frictional strength of a fault is

affected by the presence of a ductile material along the fault. In experiments to test the effect of gouge, a rock cylinder was cut at an angle of 35° to the cylinder axis, and a 2-mm-thick layer of simulated fault gouge (finely ground quartz or halite) was spread evenly on the sliding surface. The precut cylinder was jacketed and placed between the pistons of a triaxial load rig in a pressure vessel. The sample was subjected to an axial stress under a range of confining pressures, and the differential stress at which sliding initiated was determined.

Results 10-7

The stress-strain plots for experiments run with quartz gouge are shown in Figure 10-16 (from Shimamoto and Logan, 1981). When plotted on a Mohr diagram, these curves suggest that shear stress for frictional slip on gouge-coated surfaces increases with normal stress, as predicted by the general equations for sliding friction of rock. The effect of halite along a fault is shown in Figure 10-17. Under experimental conditions halite is ductile, which means that it deforms with a constant shear stress regardless of the magnitude of normal stress across the plane of shear.

Interpretation 10-7 (to be completed by the student)

(a) Using the Mohr diagram, derive the shear stress and normal stress for frictional sliding of quartz fault gouge at 8% axial shortening.

(b) Plot the shear stress and normal stress determined in part a to determine a sliding friction equation. Does it agree with the general equations for friction of rocks without gouge?

(c) Repeat part a for frictional sliding on halite.

(d) What is the coefficient of sliding friction for halite gouge?

(e) Above a confining pressure of 200 MPa frictional sliding on halite gouge requires the same shear stress as at 200 MPa. This means that the shear stress is independent of normal stress. What then is the coefficient of sliding friction for halite gouge above 200 MPa? Represent this friction criterion for halite on a Mohr diagram.

(f) Referring to Figure 10-18, if σ_3 is 300 MPa, determine the differential stress required for frictional sliding on salt. What would have been the differential stress required for slip on a plane 45° to σ_1 if the general friction equations had applied to salt?

Comments on Experiment 10-7

The Mohr circle for halite has the same diameter regardless of the confining pressure at pressures above 200 MPa. This type of behavior is modeled by the

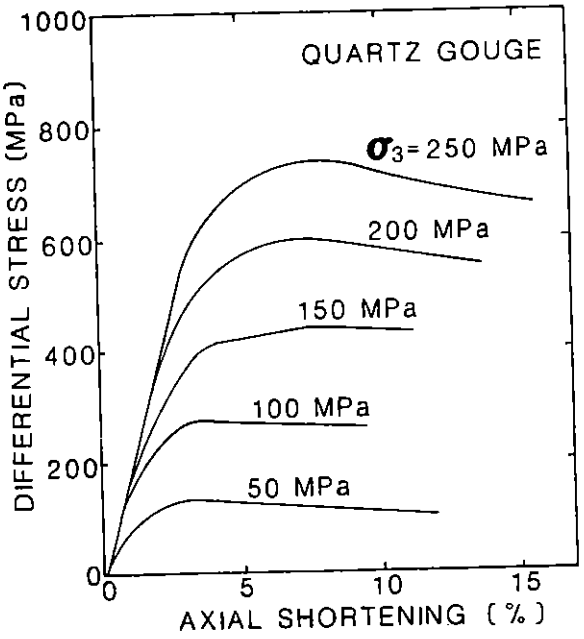

Figure 10-16. Differential stress versus axial shortening curves for the frictional sliding of quartz fault gouge as determined by Shimamoto and Logan (1981) (for Experiment 10-7) (adapted from Shimamoto and Logan, 1981).

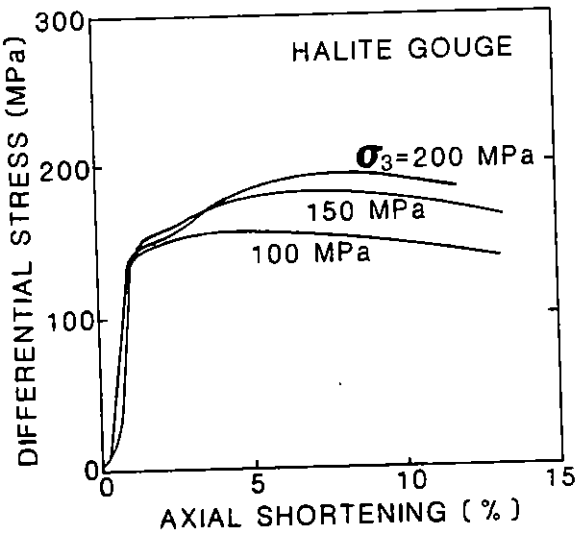

Figure 10-17. Differential stress versus axial shortening curves for the frictional sliding of halite fault gouge as determined by Shimamoto and Logan (1981) (for Experiment 10-7) (adapted from Shimamoto and Logan, 1981).

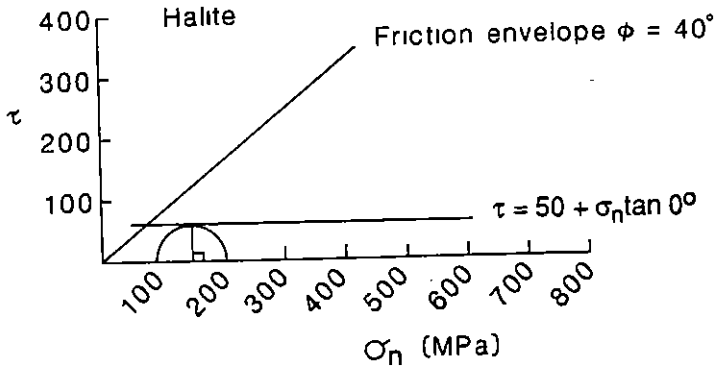

Figure 10-18. A Mohr diagram for the general fictional sliding curve for halite that is acting as a perfectly plastic material along the sliding surface (for Experiment 10-7).

Coulomb-Mohr failure criterion using a constant S_0 and $\theta = 0°$. The friction equation for salt is then

$$\tau = S_o + \sigma_n \tan 0°$$

$$S_o = 50 \text{ MPa} \qquad \text{(Eq. 10-14).}$$

The Mohr diagram describing frictional sliding on salt is presented in Figure 10-18. Such a diagram would also represent the behavior of an intact sample of rock that deforms in a perfectly plastic manner. The rock will strain at the same differential stress regardless of the confining pressure.

The significance of Equation 10-14 is that it says that for fault zones deep within the upper crust, frictional resistance to sliding is very low if the fault gouge is salt. Many thrust belts of the world, such as the Appalachian foreland, the Jura of Switzerland, and the Zagros of Iran, are wide because salt "gouge" acts to reduce frictional resistance (Davis and Engelder, 1985).

10-7 ACKNOWLEDGMENTS

We thank John Logan for a helpful review of the manuscript.

ADDITIONAL EXERCISES

1. There are several general classes of stress. All can be drawn in two dimensions using a Mohr circle. Possible stress states in the earth include:

   (a) *Tension and compression:* One principal stress is tensile and the other is compressive. This is the most likely situation for the generation of most tensile fractures (joints) within the earth's crust.
   (b) *Pure shear stress:* A special case of tension and compression, in which $\sigma_1 = -\sigma_2$, so that the planes of maximum shear stress are also planes of pure shear stress (i.e., the normal stress component is zero on these planes). This is a very unusual state of stress for the earth's crust.
   (c) *General compression:* Both principal stresses are compressive. In three dimensions this state of stress in the earth is called triaxial compression. This is the usual state of stress within the crust.
   (d) *Hydrostatic compression:* The stress across all planes is compressive and equal. Pore water within a rock can exert a state of hydrostatic compression provided that the water in the pores can communicate directly with the surface.
   (e) *Lithostatic compression:* The stress across all planes is compressive and equal to the weight of the rock on top of the point at which the measurement is made.

   Draw each of these states of stress considering the nature and relative magnitudes of the principal stresses. Note the differences in location of the center and length of the diameter of the Mohr circle for each state of stress.

2. Using the data shown in Figure 10-14 for Barre Granite, determine the shear and normal stress on the three planes shown in the cylinder of rock used for a deformation experiment if σ_1 is 100 MPa and σ_3 is 50 MPa. Calculate the answer using the appropriate equations, and derive the answer using a Mohr diagram. In this example it is important to appreciate that slip occurs on the plane whose ratio of τ to σ_n is maximum. The plane (at $\theta = 45°$) with the maximum τ did not slip because σ_n was so large that the ratio was not maximum. Likewise, the plane ($\theta = 75°$) with the minimum σ_n did not slip because τ was small.

3. Leuders Limestone is fairly weak lithology. At a confining pressure of 100 MPa, a differential stress of just over 200 MPa is required to fracture intact samples of Leuders Limestone (Fig. 10-M1a).

(a) What is the orientation of the fractures that form in Leuders Limestone?
(b) The friction envelope for Leuders Limestone is also plotted on Figure 10-M1a. Note that it is very close to the Coulomb-Mohr failure envelope. What does this relationship imply?
(c) Is there a preference for slip on an existing fracture at 34° to σ_1 over development of a new fracture at 31° to σ_1?
(d) In the paper in which Byerlee (1978) compiled friction data for many lithologies several rocks showed frictional behavior that deviated from the general friction envelope. Leuders Limestone is one of those lithologies. In Figure 10-M1b the frictional envelope defined by Equation 10-12 is plotted next to the Coulomb-Mohr failure envelope for Leuders Limestone. In this case the envelope for frictional sliding plots well above the Coulomb-Mohr failure envelope. If the general friction equations are applicable, is it ever possible for Leuders Limestone to slide on an existing fracture? If not, how will Leuders Limestone respond to elevated differential stress?
(e) Leuders Limestone is known to fail by sliding on favorably oriented preexisting fractures. What are the implications of this observation for the the acceptance of the envelope defined by Equation 10-12 (i.e., does the equation apply to all cases)?

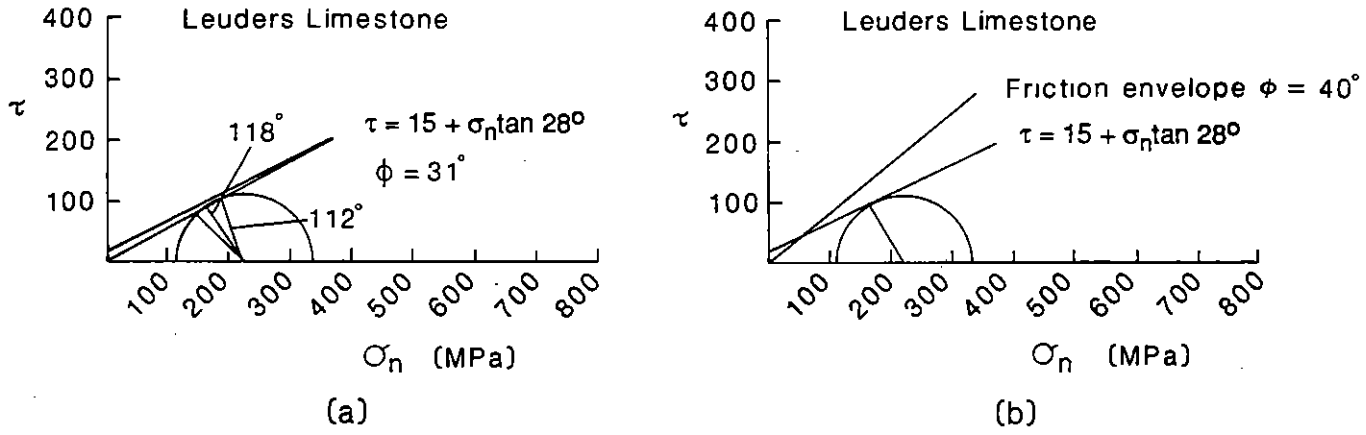

Figure 10-M1. Mohr diagrams for Leuders Limestone (for Exercise 3). (a) Diagram showing the Coulomb-Mohr failure envelope and the envelope for frictional sliding determined by Handin (1969). Circle is tangent to the Coulomb-Mohr envelope; (b) The Coulomb-Mohr failure envelope and the friction envelope defined by Equation 10-12.